



HAL
open science

Formation of Brominated Disinfection Byproducts from Natural Organic Matter Isolates and Model Compounds in a Sulfate Radical-Based Oxidation Process

Yuru Wang, Julien Le Roux, Tao Zhang, Jean-Philippe Croué

► **To cite this version:**

Yuru Wang, Julien Le Roux, Tao Zhang, Jean-Philippe Croué. Formation of Brominated Disinfection Byproducts from Natural Organic Matter Isolates and Model Compounds in a Sulfate Radical-Based Oxidation Process. *Environmental Science and Technology*, 2014, 48 (24), 10.1021/es503255j . hal-01211472

HAL Id: hal-01211472

<https://enpc.hal.science/hal-01211472v1>

Submitted on 31 Oct 2016

HAL is a multi-disciplinary open access archive for the deposit and dissemination of scientific research documents, whether they are published or not. The documents may come from teaching and research institutions in France or abroad, or from public or private research centers.

L'archive ouverte pluridisciplinaire **HAL**, est destinée au dépôt et à la diffusion de documents scientifiques de niveau recherche, publiés ou non, émanant des établissements d'enseignement et de recherche français ou étrangers, des laboratoires publics ou privés.

Copyright

1 Formation of brominated disinfection byproducts from natural
2 organic matter isolates and model compounds in a sulfate
3 radical-based oxidation process

4 *Submitted to*

5 *Environmental Science & Technology*

6 *July, 2014*

7
8 Yuru Wang, Julien Le Roux, Tao Zhang, and Jean-Philippe Croué*

9
10 Water Desalination and Reuse Center, King Abdullah University of Science and
11 Technology, Thuwal 4700, Kingdom of Saudi Arabia

12
13
14
15 * Corresponding author: Tel.: + 966 (0) 2 808 2984.

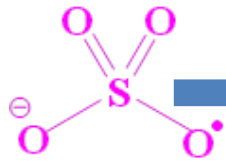
16 E-mail address: jp.croue@kaust.edu.sa

17

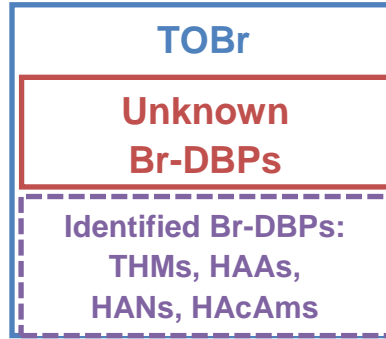
18 TOC Art

19

20



NOM



21

22

23

24

25

26

27

28

29

30

31

32

33

34

35

36

37

38

39

40 ABSTRACT

41 Sulfate radical-based advanced oxidation process (SR-AOP) has received increasing application
42 interests for the removal of water/wastewater contaminants. However, limited knowledge is
43 available on its side effects. This study investigated the side effects in terms of the production of
44 total organic bromine (TOBr) and brominated disinfection byproducts (Br-DBPs) in the presence
45 of bromide ion and organic matter in water. Sulfate radical was generated by heterogeneous
46 catalytic activation of peroxymonosulfate. Isolated natural organic matter (NOM) fractions as
47 well as low molecular weight compounds were used as model organic matter. Considerable
48 amounts of TOBr were produced by SR-AOP, where bromoform (TBM) and dibromoacetic acid
49 (DBAA) were identified as dominant Br-DBPs. In general, SR-AOP favored the formation of
50 DBAA, which is quite distinct from bromination with HOBr/OBr⁻ (more TBM production). SR-
51 AOP experimental results indicate that bromine incorporation is distributed among both
52 hydrophobic and hydrophilic NOM fractions. Studies on model precursors reveal that low
53 molecular weight acids are reactive TBM precursors (citric acid > succinic acid > pyruvic acid >
54 maleic acid). High DBAA formation from citric acid, aspartic acid, and asparagine was observed;
55 meanwhile aspartic acid and asparagine were the major precursors of dibromoacetonitrile and
56 dibromoacetamide, respectively.

57

58

59

60

61

62

63 INTRODUCTION

64 Bromide ion is a ubiquitous component of natural waters and its concentration significantly
65 varies depending on the water source.¹⁻³ When water is disinfected with chlorine, ozone or
66 chlorine dioxide, bromide ion can be quickly oxidized to hypobromous acid (HOBr), which
67 subsequently reacts with natural organic matter (NOM) to yield brominated disinfection
68 byproducts (Br-DBPs) in an analogous way to hypochlorous acid (HOCl). Elevated bromide
69 levels in source waters have been reported to induce a significant shift in speciation to Br-DBPs,
70 attributed to HOBr being a more efficient substitution agent in comparison with HOCl.⁴ It has
71 been shown that Br-DBPs are generally more cyto- and genotoxic than their chlorinated
72 analogues.⁵

73 In recent years, sulfate radical ($\text{SO}_4^{\bullet-}$)-based advanced oxidation processes (SR-AOPs) have
74 gained great scientific and technological interests for the decontamination of groundwater,
75 surface water and industrial wastewaters. Sulfate radical with a high standard reduction potential
76 (2.5 – 3.1 V) can react with a broad spectrum of organic contaminants at near diffusion-
77 controlled limits.⁶ $\text{SO}_4^{\bullet-}$ can be generated through the activation of persulfates (i.e.,
78 peroxymonosulfate (PMS) and peroxydisulfate (PDS)) by alkaline, UV, heat, or transition
79 metals.⁷⁻¹⁰ Compared to hydrogen peroxide, persulfates in solid state are relatively stable,
80 therefore favoring storage and transportation. The strong oxidative capacity, relative stable
81 nature, and high aqueous solubility of its precursor compounds (i.e., PMS and PDS), in
82 combination with a variety of $\text{SO}_4^{\bullet-}$ -generating techniques, make sulfate radical an excellent
83 alternative for eliminating recalcitrant organic pollutants. Recently, promising treatment
84 efficiency of SR-AOPs for waters with various challenging matrices (e.g., landfill leachate) has

85 been reported.¹¹⁻¹³ Moreover, there has been interest in the application of SR-AOPs as alternative
86 disinfectants.¹⁴

87 Similarly to hydroxyl radical, the inorganic constituents of waters are usually competing
88 scavengers of $\text{SO}_4^{\bullet-}$. Halide ions are known as important sink of $\text{SO}_4^{\bullet-}$. Particularly, bromide ion
89 is of special concern because its reactivity with $\text{SO}_4^{\bullet-}$ is approximately 13-fold higher than that of
90 chloride ion.^{15, 16} In the presence of bromide ions, bromine atom (Br^{\bullet}) formation by $\text{SO}_4^{\bullet-}$
91 oxidation is quite fast. Once Br^{\bullet} is formed, it quickly reacts with bromide ion to produce
92 dibromine anion radical ($\text{Br}_2^{\bullet-}$).¹⁷ Besides, Br^{\bullet} and $\text{Br}_2^{\bullet-}$ can also undergo a series of reactions
93 with Br^- and H_2O , leading to the generation of $\text{BrOH}^{\bullet-}$ and HOBr/OBr^- (see [Table S1](#) of the
94 Supporting Information (SI)).¹⁷⁻²¹ Direct reaction of bromide ion with the monosubstituted
95 peroxide precursor of $\text{SO}_4^{\bullet-}$ (i.e., PMS) also occurs, however, the rate of active bromine
96 formation is extremely low when PMS is used alone without activation ([Figure S1](#)).²² In water,
97 these chain reactions involving reactive bromine species (i.e., Br^{\bullet} , $\text{Br}_2^{\bullet-}$, $\text{BrOH}^{\bullet-}$, and
98 HOBr/OBr^-) can be terminated by reacting with NOM to form brominated byproducts, which
99 poses one of the primary issues of concern for the real water/wastewater application of SR-
100 AOPs.

101 To date, no information is available about bromine-incorporation into organic matter from
102 bromide-containing water during SR-AOPs. Therefore, the objectives of this research were to
103 investigate the formation and speciation of regulated and emerging DBPs with respect to NOM
104 properties, and to study and compare bromine-incorporation by SR-AOPs with bromination by
105 HOBr/OBr^- . Brominated trihalomethanes (THMs), haloacetic acids (HAAs), and
106 haloacetonitriles (HANs) are the major Br-DBPs of concern in this study. Total organic bromine
107 (TOBr) was used to evaluate the total incorporation of bromine into organic molecules.

108 Moreover, a range of structurally diverse model compounds including six amino acids (Group I),
109 three phenolic compounds (Group II), and six carboxylic acids (Group III) which represent
110 important moieties of NOM were tested to identify significant precursors of Br-DBPs and
111 TOBr.²³ Amino acids featuring high levels of organic nitrogen may promote nitrogenous
112 disinfection byproducts (N-DBPs) formation. Haloacetamides (HAcAms), an emerging class of
113 N-DBPs, were therefore monitored for experiments involving amino acids. The CuFe₂O₄
114 activated PMS process was employed to generate SO₄^{•-}, rather than UV/PMS or UV/PDS, to
115 avoid any interference from UV irradiation.²⁴

116 MATERIALS AND METHODS

117 **Materials.** A detailed description of reagents and preparation procedures of CuFe₂O₄ spinel
118 catalyst and bromine stock solution is provided in [Text S1](#) (SI).

119 **NOM Samples and Selection of Model Compounds.** Four previously isolated
120 NOM fractions were employed in this study ([Table S2](#), SI). Three hydrophobic NOM fractions
121 (i.e., hydrophobic acids or HPOA obtained from base desorption, hydrophobic or HPO isolated
122 with acetonitrile/water desorption) showing very different chemical composition were selected:
123 SR HPOA isolated from the Suwannee River (Georgia, USA); SPR HPOA isolated from the
124 South Platte River (Colorado, USA) and CR HPO obtained from Colorado River (California/LA
125 Verne, USA). The hydrophilic acid and neutral fraction (BR HPIA+N) isolated from Blavet
126 River (Côte D'Armor, France) was also used in this work. NOM fractions were isolated using
127 two slightly different comprehensive isolation protocols described elsewhere.²⁵ Three groups of
128 model compounds representing functional moieties of NOM were selected as NOM surrogates.
129 Group I consisted of six amino acids (i.e., asparagine, glutamic acid, phenylalanine, tryptophan,
130 tyrosine, and aspartic acid). Group II included three phenolic compounds (i.e., phenol,

131 hydroquinone, and salicylic acid). Six carboxylic acids (i.e., citric acid, oxalic acid, malonic acid,
132 succinic acid, maleic acid, and pyruvic acid) were selected as group III to represent low
133 molecular weight acids. Structures and physicochemical properties of the model compounds are
134 presented in [Table S3](#) (SI).

135 **Experimental Procedure.** Experiments were conducted in duplicate or triplicate at
136 room temperature (20 ± 2 °C) in 250 mL capped amber bottles (individual bottle per contact time)
137 under headspace-free conditions. NOM isolate experiments were performed at a concentration of
138 $5\text{-}7$ mg L⁻¹ (final DOC content of 2.2 to 2.7 mg L⁻¹ was verified by TOC analyzer) in the
139 presence of 2 mg L⁻¹ bromide (25 μM Br⁻) buffered with 10 mM tetraborate, unless otherwise
140 indicated. Reactions with model compounds were conducted with 50 μM individual molecule
141 solutions in the presence of 4 mg L⁻¹ bromide (50 μM Br⁻) buffered with 10 mM tetraborate.
142 Nitric acid and/or sodium hydroxide were used to adjust the initial pH of the solutions. For SO₄^{•-}-
143 based tests, the reaction was initiated by adding an appropriate amount of CuFe₂O₄ spinel
144 catalyst and PMS (Sigma Aldrich, KHSO₅·0.5KHSO₄·0.5K₂SO₄) stock solution. The
145 CuFe₂O₄/PMS system generates SO₄^{•-} as the major radical species and the sulfate radical yield
146 ratio from PMS was approximately 1 mol per mol.²⁴ The bottles were immediately capped and
147 placed in a shaker (IKA[®] KS 260) at a speed of 500 rpm to maintain complete homogeneity
148 throughout the reaction. Samples were withdrawn at specific time intervals, immediately
149 quenched with excess sodium nitrite, and then filtered through 0.45 μm glass fiber syringe filters
150 before analysis. Bromination was conducted as a comparison by dosing a predetermined amount
151 of HOBr/OBr⁻ into the same amount of NOM isolates and model compound solutions buffered
152 with 10 mM tetraborate in 250 mL amber bottles without headspace.

153 **Analytical Methods.** *NOM solution analyses.* Dissolved organic carbon (DOC) content
154 was measured by a Shimadzu TOC-Vcsh Analyzer. UV absorbance at 254 nm was recorded
155 using a Shimadzu UV-2550 UV-VIS spectrophotometer. A liquid chromatography-organic
156 carbon detector (LC-OCD Model 8, DOC-LABOR, Germany) with a size exclusion
157 chromatography column was employed to compare NOM compositions. Three-dimensional
158 fluorescence excitation - emission matrices (FEEM) were obtained using an Aqualog® CDOM
159 Fluorometer (Horiba Scientific, Japan). Further details with respect to LC-OCD and FEEM
160 measurements are presented in [Text S2 \(SI\)](#).

161 *Brominated organic compounds and residual oxidant.* Samples for TOBr analysis were
162 enriched through adsorption on activated carbon column using a TOX sample preparatory unit
163 (TXA-03, Mitsubishi Chemical Analytech Co., Ltd, Japan). TOBr was then transformed into
164 hydrogen halide under high-temperature (950 °C) combustion of the activated carbon for at least
165 30 min via an AOX-200 adsorbable halogen analyzer, and then collected in Milli-Q water as
166 bromide ion. Off-line quantification of bromide ion was performed by ion chromatography
167 (Dionex ICS-1600) equipped with a conductivity detector and a Dionex IonPac® AS-15 column
168 (2 × 250 mm), using a 30 mM KOH solution at a flow rate of 0.4 mL min⁻¹ as mobile phase. The
169 obtained Br⁻ concentration was used to calculate the concentration of TOBr (as µg L⁻¹ Br⁻).
170 During bromination experiments, residual bromine was monitored at the time of sampling by
171 DPD colorimetric method. Residual PMS was determined using colorimetric method after
172 reacting with Co²⁺ and ABTS to form a colored ABTS radical cation (further details in [Text S3](#),
173 SI).

174 *Br-DBPs analysis.* Samples for the analysis of THMs/HAAs were extracted with methyl tert-
175 butyl ether (MTBE) within 1 h after quenching based on the EPA Method 551 and 552,

176 respectively. HAcAms were extracted with ethyl acetate following a similar method to EPA
177 Method 551. THMs, HANs, and HAcAms were quantified on a gas chromatography (Agilent
178 7890A) equipped with an electron capture detector (GC-ECD), while MTBE extracts for HAAs
179 were analyzed on an Agilent 7890A GC equipped with Agilent 5975C inert XL MSD with Triple
180 Axis Detector (GC-MSD). DBPs were separated on a DB-1701 (30 m × 250 μm × 0.25 μm)
181 capillary column. Analytical details are provided in the SI ([Text S3](#)).

182 RESULTS AND DISCUSSION

183 **Characteristics of NOM Isolates.** The NOM isolates exhibited a wide range of
184 SUVA₂₅₄ values ([Table S2](#)). SR HPOA showed the highest SUVA₂₅₄ (4.97 L mg⁻¹ m⁻¹),
185 indicating a high degree of aromaticity, followed by SPR HPOA (3.11 L mg⁻¹ m⁻¹) and CR HPO
186 (2.08 L mg⁻¹ m⁻¹). BR HPIA+N showed the lowest SUVA₂₅₄ (1.27 L mg⁻¹ m⁻¹), which is
187 characteristic of low content of aromatic moieties. Our previous works²⁵ indicated that SR
188 HPOA is characterized by the predominance of fulvic acid structures derived from lignins and
189 tannins (high aromatic/phenolic carbon and carboxyl group contents) and CR HPO mainly
190 incorporates fulvic acid structures derived from terpenoids (lower aromatic carbon and phenolic
191 content, higher methyl group content) incorporating abundant polysaccharides moieties. SPR
192 HPOA showed an intermediate composition with both types of aromatic structures well
193 represented.²⁵ In general, hydrophilic acids plus neutral NOM such as BR HPIA+N can be
194 described as a mixture of aliphatic hydroxy acids (e.g., low molecular weight acids), N-
195 acetylaminosugars, neutral carbohydrates, and neutral peptides.²⁵ These differences in
196 composition between the four NOM fractions are in good agreement with the additional
197 structural information obtained by LC-OCD and FEEM analyses ([Text S3 and Figures S2 to S4](#),
198 SI).

199 **Bromine-incorporation into NOM Isolates.** Preliminary experiments with SR
200 HPOA were conducted to investigate the formation kinetics of TOBr and Br-DBPs from
201 bromide-containing water by SR-AOP. Recent studies have shown that $\text{SO}_4^{\bullet-}$ can lead to
202 complete conversion of Br^- to BrO_3^- in ultrapure water via HOBr/OBr^- as an intermediate path.^{2,}
203 ²⁶ However, no bromate formation was observed in this study in the presence of NOM. Moreover,
204 the CuFe_2O_4 catalyst had negligible impacts on the UV absorbance at 254 nm and TOC of NOM
205 isolates, suggesting insignificant adsorption of NOM on the catalyst (data not shown). [Figure 1](#)
206 illustrates TOBr and Br-DBPs evolution profiles by SR-AOP in the presence of 25 μM Br^- at pH
207 7.5. TOBr was rapidly formed within the first 4 h, where fast decomposition of PMS (> 70%)
208 was observed. After 4 hours, TOBr concentration slowly decreased throughout the duration of
209 the experiment (24 h), which is probably due to reactions of sulfate radical with TOBr
210 components. Bromoform (TBM) formation showed a similar trend as TOBr, suggesting that
211 TBM can be oxidized by the sulfate radicals remaining in the system, which was confirmed by
212 additional experiments ([Figure S5](#)). Yields of both dibromoacetic acid (DBAA) and
213 monobromoacetic acid (MBAA) gradually increased with reaction time. As opposed to TBM,
214 HAAs were not decomposed at longer reaction times. Low levels (< 4 $\mu\text{g L}^{-1}$) of
215 bromochloroacetonitrile (BCAN) and dibromochloromethane (DBCM) were produced due to the
216 presence of trace chloride in the potassium bromide salt used to prepare the solutions.

217 [Figures 2-4](#) present the influence of PMS concentration, bromide ion concentration, and
218 solution pH on the formation and speciation of TOBr and Br-DBPs by SR-AOP. In all cases
219 TBM and DBAA were the dominant identified Br-DBPs. TOBr and HAAs increased with
220 increasing PMS dosage, while the formation of TBM exhibited an increasing and then a
221 decreasing pattern because of its destruction with excess sulfate radicals. Increasing bromide

222 concentration enhanced the formation of TOBr, TBM, and DBAA (Figure 3), which was
223 expected, as an increase in $[\text{Br}^-]$ led to a greater concentration of reactive bromine radical species
224 in the system. As shown in Figure 4, the formation of both TOBr and identified Br-DBPs was
225 highly pH-dependent. TOBr and DBAA gradually increased with increasing pH until reaching a
226 maximum at pH 7.5 and then rapidly decreased as pH was further increased to 9.5, which is
227 possibly related to the transformation of $\text{SO}_4^{\bullet-}$ to hydroxyl radical through the reaction with OH^- .
228 The high efficiency of $\text{CuFe}_2\text{O}_4/\text{PMS}$ system at neutral pH was discussed in detail in a previous
229 study.²⁴ The significant reduction of TOBr and DBAA at higher pH is also likely related to the
230 non-radical self-dissociation pathway of PMS in alkaline conditions.²⁷ Besides, hydrolysis of
231 DBAA at $\text{pH} > 8.0$ is believed to be another reason responsible for its reduced concentration at
232 basic pH.²⁸ TBM formation increased with increasing pH, which is consistent with the
233 commonly accepted explanation that base-catalyzed hydrolysis mechanisms play a significant
234 role in THM formation.²⁹ This pH dependence of DBAA and TBM formation from NOM by SR-
235 AOP follows the behavior expected for chlorination/bromination of NOM, suggesting that
236 sulfate radical-induced formation of Br-DBPs showed some similarities compared to that of
237 chlorination/bromination. As a result, further studies were conducted to fully address the
238 differences and similarities between the two processes.

239 Figure 5 illustrates the formation and speciation of TOBr and Br-DBPs from various NOM
240 isolates by SR-AOP in the presence of $25 \mu\text{M Br}^-$ at pH 7.5 and for a contact time of 2 h in
241 comparison with bromination (a HOBr/OBr^- concentration of $25 \mu\text{M}$). The comparison was
242 conducted to test if the bromination trend of these reactive bromine species generated in SR-
243 AOP is different from that of HOBr/OBr^- . Considerable formation of TOBr from NOM isolates
244 by sulfate radical oxidation of bromide-containing water was observed, ranging from 56 - 107 μg

245 $\text{mg}^{-1} \text{C}$ (Figure S6). On a molar basis, about 6.5 - 12.2% (Figure 5a) of the initial bromide was
246 transformed to TOBr. Nevertheless, SR-AOP produced much less TOBr than the bromination
247 process. Approximately 8.5 - 25% of initial bromine was incorporated into TOBr, likely due to
248 (1) bromine being a preferable substituting agent⁴ and (2) possible subsequent decay of
249 brominated compounds by sulfate radical in SR-AOP system.² It is known that identified DBPs
250 only account for a fraction of the total organic halogen (TOX). In fact, approximately 50% of the
251 TOX from chlorination of natural waters remains unknown,^{5, 30-32} while over 70% formed by
252 chloramines has not been identified.^{32, 33} In the present study, quantified Br-DBPs only
253 constituted 22 - 33% of TOBr during SR-AOP, compared to 28 - 48% in bromination (Figure
254 5a). Speciation analysis revealed that DBAA was the predominant Br-DBPs during SR oxidation,
255 accounting for $90 \pm 6\%$ of HAAs and $54 \pm 6\%$ of total identified Br-DBPs by weight, followed
256 by TBM which contributed to $75 \pm 3\%$ of the THMs and $31 \pm 3\%$ of total identified Br-DBPs. In
257 contrast, NOM isolates were more susceptible to the formation of Br-THMs upon bromination.
258 TBM was by far the major contributor of total identified Br-DBPs (63 - 86% on a weight basis)
259 upon bromination, while DBAA and TBAA contributed to 5.2 - 10.4% and 3.2 - 5.3%,
260 respectively (Figure 5b and 5c). Besides, bromination tended to incorporate more bromine into
261 HAAs to form mainly DBAA and TBAA, while SR-AOP yielded mainly DBAA and MBAA (to
262 a lesser extent) with negligible TBAA formation, indicating again a different trend in Br-DBPs
263 formation from active bromine species formed in SR-AOP as compared with bromination.

264 For both SR-AOP and bromination, the formation of TOBr and Br-DBPs among different
265 types of NOM isolates exhibited distinct variation, which could be related to the different NOM
266 properties and their reactivities towards the oxidants. TOBr and Br-DBPs formation correlated
267 well to the SUVA_{254} values of the three hydrophobic NOM isolates during SR-AOP.

268 Interestingly the hydrophilic NOM isolate (i.e., BR HPIA+N) with the lowest SUVA₂₅₄ formed
269 high amounts of both TOBr and Br-DBPs similar to those formed from SR HPOA (Figure 5a).

270 These results demonstrate that SR-AOP favors the formation of DBAA in comparison to
271 bromination which tends to produce more TBM. The DBAA yields from various NOM isolates
272 during SR-AOP were 2.4 - 5.84 times higher than those from bromination. The hydrophilic
273 fraction as well as hydrophobic acid with the highest SUVA₂₅₄ value were the dominant sources
274 of TOBr and Br-DBPs during SR-AOP, while good correlations ($R^2 > 0.81$) were observed
275 between aromaticity of NOM and Br-DBP formation during bromination. The significant
276 differences in distribution and speciation pattern of Br-DBPs upon SR-AOP and bromination
277 suggest that sulfate radical-induced DBPs formation involves different reaction mechanisms as
278 compared to bromination. In the SR-AOP system, both $SO_4^{\bullet-}$ and bromine radicals (e.g., Br^{\bullet} and
279 $Br_2^{\bullet-}$) can react with organic compounds via abstraction of hydrogen, addition to unsaturated
280 compounds or one-electron oxidation.¹⁵ As such, multiple pathways could be involved in the
281 formation of TOBr and Br-DBPs by SR-AOP. To further understand the importance of precursor
282 characteristics and the DBPs formation mechanisms in SR-AOP system, a broad spectrum of
283 model compounds were tested as precursors.

284 **Formation of TOBr and Br-DBPs from Model Compounds.** Table 1

285 summarizes the incorporation of 50 μ M bromide ion (i.e., 4 mg L⁻¹) into 50 μ M model
286 compounds by SR-AOP (100 μ M PMS and 50 mg L⁻¹ CuFe₂O₄) at pH 8 and 24 h of contact
287 time. Bromination of 50 μ M model compounds by 50 μ M HOBr at pH 8 was tested for
288 comparison. Results for 2 h of reaction were also provided in Table S4 (SI). Consistent with the
289 observation of bromine incorporation into NOM isolates, SR-AOP induced higher yields of
290 DBAA and MBAA for nearly all the model precursors in comparison to bromination.

291 Particularly, LMW acids (Group III) were certainly the most important precursors of TBM
292 during SR-AOP, while TBM yields from amino acids (Group I) and phenolic compounds (Group
293 II) were minimal. Upon SR-AOP and bromination, TBAA mainly originated from LWM acids
294 and phenolic compounds, respectively. For the SR-AOP system, TBM formation from each
295 aliphatic carboxylic acid predominated over the other identified Br-DBPs, whereas DBAA was
296 the major species from amino acids and phenolic compounds. Formation of N-DBPs was
297 observed by both SR-AOP and bromination of amino acids, although generally to a small extent
298 except for asparagine.

299 Among the studied model compounds, citric acid (a very HPI acid), was the most reactive Br-
300 DBPs precursor upon SR-AOP, yielding the highest amounts of TBM ($1144.3 \mu\text{g L}^{-1}$), DBAA
301 ($434.6 \mu\text{g L}^{-1}$), and MBAA ($85.3 \mu\text{g L}^{-1}$). More than 35.8% of initial bromide ion was
302 incorporated into TOBr, where the identified Br-DBPs accounted for nearly 100% of TOBr.
303 Bromination of citric acid also yielded comparable TBM and to a lesser degree DBAA after 24 h.
304 However, TBM formation from bromination was much slower as only 14.0% was produced
305 within 2 h, whereas more than 68.8% of the 24 h TBM yield was formed in 2 h by SR-AOP.
306 Sulfate radicals are known to efficiently react with most aliphatic carboxylic acids, leading to
307 oxidative decarboxylation of these compounds.³⁴ Besides, reaction rate constants of $\text{SO}_4^{\bullet-}$
308 scavenging by carboxylate ions are significantly higher than their corresponding carboxylic
309 acids due to the fact that the former proceeds by one electron transfer from the carboxylate group
310 to $\text{SO}_4^{\bullet-}$ and the latter via hydrogen abstraction from C-H bond.³⁵ Consequently, decarboxylation
311 of aliphatic carboxylic acids by $\text{SO}_4^{\bullet-}$ through one electron transfer is favored in this study as
312 most LMW acids were deprotonated into carboxylate anion at pH 8 (see Table S3 for the pK_a
313 values). For citric acid, $\text{SO}_4^{\bullet-}$ first abstracts one electron from the carboxylate group of β -carbon

314 followed by the loss of CO₂ and the formation of a corresponding C-centered radical
315 (HOC•(CH₂COO⁻)₂) which then converts the hydroxyl group of the β-carbon to a more stable
316 form of keto group. The resulting 3-oxopentanedioic acid (HOOC-CH₂-C(O)-CH₂-COOH), an
317 aliphatic β-keto acid, favors rapid halogenation at the two enolizable methylene groups doubly
318 activated by adjacent carbonyl groups.³⁶ Subsequent decarboxylation/hydrolysis or oxidation of
319 the ketone gives rise to substantial TBM, DBAA, and MBAA formation. Bromination of 3-
320 oxopentanedioic acid at pH 8 was reported to be relatively fast.³⁷ As such, oxidative
321 decarboxylation of citric acid and subsequent transformation into 3-oxopentanedioic acid are
322 believed to be the rate-limiting step responsible for the slower TBM formation kinetics of citric
323 acid by bromination as compared to SR-AOP.

324 Pyruvic acid, an α-keto acid, was another important TBM precursor by SR-AOP. TBM
325 accounted for 95% of the TOBr formed followed by a small amount of DBAA. Although to a
326 lesser extent, bromination of pyruvic acid also yielded considerable amount of TBM.
327 Chlorination of pyruvic acid was reported to proceed via dominated oxidation pathway (>
328 98.5%), yielding TCAA as major byproduct.³⁸ In this study, the electrophilic substitution
329 pathway dominates given the prevailing TBM yields. The reaction pathway discrepancy between
330 SR-AOP/bromination and chlorination is likely due to a higher reactivity of bromine species than
331 chlorine in halogenating reactions. It is reasonable that α-hydrogens in methyl group of pyruvic
332 acid undergo three successive halogenations upon the attack by bromine radicals or bromine to
333 give a tribromopyruvic acid (CBr₃-C(O)-COOH). Subsequent hydrolysis of this intermediate
334 releases TBM and oxalic acid. Based on the formation of DBAA by SR-AOP, decarboxylation
335 pathway that converts pyruvic acid to acetaldehyde (CH₃CHO) should also occur. The resulting
336 acetaldehyde favors halogenation at α-hydrogens, further oxidation leading to DBAA.

337 8.1% of initial bromide was incorporated into TOBr formed from maleic acid by SR-AOP, and
338 TBM contributed to 43.6% of TOBr. In contrast, bromination showed different patterns of
339 speciation with 19.1% bromine being converted into TOBr, while TBM accounted for only 3.76%
340 of TOBr. The significantly higher TBM formation by SR-AOP is believed to result from the
341 preference of sulfate radical on oxidizing unsaturated carbon bonds.³⁹ Initially, the attack of
342 $\text{SO}_4^{\bullet-}$ on the carbon-carbon double bond of maleic acid leads to the formation of oxobutanedioic
343 acid ($\text{HOOC-C(O)-CH}_2\text{-COOH}$) through hydroxylation along with isomerization.
344 Decarboxylation of oxobutanedioic acid occurs yielding pyruvic acid, which eventually leads to
345 the formation of TBM upon further reactions. It is also probable that oxobutanedioic acid, which
346 is also an aliphatic β -keto acid, contains an activated methylene group especially susceptible to
347 halogenation. After halogenation, decarboxylation likely occurs yielding a dibromopyruvic acid,
348 which can undergo halogenation followed by hydrolysis to yield TBM. Bromination of maleic
349 acid is known to proceed via anti-addition reaction on alkene group to form a stable mixture of
350 dibromomaleic acid enantiomers,⁴⁰ which would explain the relatively higher TOBr and
351 considerably lower TBM formation observed.

352 For the three saturated dicarboxylic acids (i.e., oxalic acid, malonic acid, and succinic acid)
353 subjected to SR-AOP, both TBM and DBAA yields increased with increasing carbon chain
354 length. Insignificant substitution occurred on oxalic acid upon SR-AOP with less than 3.7% of
355 bromine incorporated into TOBr. Oxalic acid being the simplest dicarboxylic acid with its two
356 carbon atoms in the maximum oxidation state, decarboxylation proceeding twice to yield two
357 carbon dioxides should be the dominating reaction pathway, supported by the conclusion of
358 Zhang et al.²⁴ Upon attack by sulfate radical, malonic acid also undergoes decarboxylation to
359 form acetic acid which can be hardly halogenated due to the inductive effect of carbonyl group

360 and the absence of an electron donating alkyl group. In this study, succinic acid was the second
361 most significant TBM precursor upon SR-AOP (see [Table 1](#)) with more than 14.4% of initial
362 bromine being converted into TBM. It is likely that decarboxylation of succinate occurs twice
363 followed by complete halogenation to yield two TBM. For bromination, both oxalic acid and
364 succinic acid were characterized by a low bromine demand (see [Table S5](#)), and low TOBr and
365 TBM formation, where only 2.3% and 1.5% of bromine was incorporated into TOBr,
366 respectively. Similar findings were also observed when oxalic acid was subjected to
367 chlorination.⁴¹ Bromination of malonic acid led to nearly no TBM formation, but yielded
368 significant amount of DBAA with 9% of bromine being incorporated into DBAA after 24 h and
369 more than 71% being formed within the first 2 h. This high DBAA formation can be explained
370 by the presence of an α -carbon flanked by two adjacent carbonyl functional groups enhancing
371 electrophilic substitution. Accordingly, malonic acid undergoes α -bromination twice to give a
372 dibromomalonic acid which subsequently decarboxylates to DBAA.

373 Upon SR-AOP, asparagine was a predominant precursor of dibromoacetamide (DBAcAm)
374 ($117.4 \mu\text{g L}^{-1}$ at 24 h) which along with DBAA ($74 \mu\text{g L}^{-1}$ at 24 h) were the major Br-DBPs
375 generated. DBAcAm yield ($1068.6 \mu\text{g L}^{-1}$) from bromination of asparagine was substantial with
376 over 19% of initial bromine being incorporated into DBAcAm, which was more than 8 times of
377 that from SR-AOP. DBAA and DBAN were also produced from bromination of asparagine
378 ($233.3 \mu\text{g L}^{-1}$ and $112.9 \mu\text{g L}^{-1}$, respectively). DBAcAm was formed to a considerably higher
379 extent by bromination. Besides, asparagine exhibited a very fast DBAcAm formation rate upon
380 bromination with nearly 100% being formed within 2 h, while DBAN slowly increased from
381 $14.9 \mu\text{g L}^{-1}$ at 2 h to $112.9 \mu\text{g L}^{-1}$ at 24 h. This result suggests that the majority of DBAcAm is
382 not likely a result of the dihaloacetonitrile (i.e., DBAN in this study) hydrolysis pathway.⁴² In

383 contrast, the side-chain amide group of asparagine plays a key role in DBAcAm formation,
384 similarly to the mechanism of asparagine chloramination proposed by Huang et al.⁴³ Compared
385 to bromination, the lower DBAcAm formation from asparagine by SR-AOP may result from the
386 oxidation of the side-chain amide nitrogen group by sulfate radical and bromine radicals ($\text{Br}^\bullet/\text{Br}$
387 (2.00 V)) due to their high redox potential. Small amounts of bromoacetamide (BAcAm) were
388 generally detected from amino acids subjected to SR-AOP with asparagine as the major
389 precursor. However, this was not observed during bromination. Aspartic acid, selected as a
390 hydrophilic surrogate, was the second most reactive precursor of DBAA ($198.3 \mu\text{g L}^{-1}$) and
391 MBAA ($18.3 \mu\text{g L}^{-1}$) and the principal contributor of DBAN ($29.2 \mu\text{g L}^{-1}$) as a result of SR-AOP.
392 Similar formation patterns were also observed from chlorination of aspartic acid.⁴¹ The relatively
393 high formation of DBAA can be explained by the preferential formation of 3-oxopropanoic acid
394 at pH 8 which is an aliphatic β -keto acid compound and a moiety known to have high
395 dihaloacetic acid formation potential.^{37, 44} Bromination of amino acids exerted a significant
396 bromine demand, where nearly 100% bromine was consumed within 2 h (Table S5). Asparagine
397 and tyrosine exhibited a high halogenation efficiency with 39.4% and 32.6% of initial bromine
398 being converted into TOBr in 24 h, respectively, while the other amino acids were characterized
399 by lower TOBr formation (< 6%).

400 Model compounds with phenolic groups including tyrosine, phenol, and salicylic acid were
401 major precursors of TOBr upon both SR-AOP and bromination. This would be attributed to the
402 electron-donating effect of hydroxyl group attached to the aromatic ring, therefore facilitating the
403 electrophilic aromatic substitution by both reactive bromine radicals and bromine. For Group II
404 in the SR-AOP system, DBAA was the major identified Br-DBPs followed by TBM and MBAA,
405 while no formation of TBAA was observed (Table 1). On the other hand, bromination of model

406 compounds with phenolic groups produced considerable amounts of TBM followed by small
407 amounts of TBAA and DBAA.

408 **Environmental Significance.** It is proved in our previous study²⁴ that PMS forms inner-
409 sphere coordination (i.e., specific adsorption, a strong surface interaction which is not influenced
410 by ionic strength) with the surface metal sites of CuFe_2O_4 . In excess of PMS, one can expect that
411 the bromine species generated in the solution would have limited access to the metal sites of the
412 catalyst because these sites are already occupied by PMS. Figure 1a shows that bromine
413 incorporation into the organic structure (i.e., bromination) finished within 4 hours, while the
414 remaining PMS concentration in the solution was still above $10\ \mu\text{M}$. Therefore, PMS was in
415 excess during the major bromination reaction. Although this study is based on the specific
416 CuFe_2O_4 -induced sulfate radical generation process, the result can still largely represent the
417 bromination trend of organic matter in SR-AOPs. Our study reveals that $\text{SO}_4^{\bullet-}$ based-AOPs
418 produces brominated byproducts including regulated and emerging Br-DBPs when applied to
419 waters containing bromide ions. At bromide concentrations relevant to natural environment (i.e.,
420 $2.5 - 6.5\ \mu\text{M}$) our results showed that significant amount of TOBr (i.e., $25 - 50\ \mu\text{g mg}^{-1}\ \text{C}$) with
421 bromoform and dibromoacetic acid as the major identified Br-DBP species (i.e., $3.5 - 6$ and $2 - 7$
422 $\mu\text{g mg}^{-1}\ \text{C}$) can be produced from sulfate radical within 2 hours at pH 7.5. When applied as a
423 decontamination strategy for natural waters (i.e., bromide containing ground or surface waters
424 with DOC content ranging from 2 to $10\ \text{mg L}^{-1}$), the potential risk of producing substantial
425 amount of regulated and non-regulated Br-DPBs from sulfate radical oxidation should be
426 considered. In the case of potable water production, the formed Br-DPBs from sulfate radical
427 reaction (i.e., can be viewed as a polishing treatment step) may contribute for a significant part
428 to the DBP content obtained after final disinfection. Moreover, special attention should be given

429 to those containing a substantial fraction of hydrophilic NOM species not easily removed by
430 conventional water treatment process (e.g., coagulation). Groundwater is also usually
431 characterized by a considerable content of hydrophilic organic matter.⁴⁵ Particularly, SR-AOPs
432 have already been applied in ground water remediation.⁴⁶ Further investigation is required to
433 elucidate the importance of other halide ions on the formation of halogenated byproducts by SR-
434 AOPs and to monitor the evolution of active halide species as well.

435 ASSOCIATED CONTENT

436 **Supporting Information.** Detailed descriptions of materials and methods as well as
437 supporting tables and figures are included in the SI. This information is available free of charge
438 via the Internet at <http://pubs.acs.org>.

439 ACKNOWLEDGEMENTS

440 Research reported in this work was supported by the King Abdullah University of Science and
441 Technology (KAUST) and the Fundamental Research Funds for the Central Universities
442 (GK201402031).

443 REFERENCES

- 444 1. Magazinovic, R. S.; Nicholson, B. C.; Mulcahy, D. E.; Davey, D. E., Bromide levels in natural waters:
445 its relationship to levels of both chloride and total dissolved solids and the implications for water
446 treatment. *Chemosphere* **2004**, *57*, (4), 329-335.
- 447 2. Fang, J. Y.; Shang, C., Bromate Formation from Bromide Oxidation by the UV/Persulfate Process.
448 *Environ. Sci. Technol.* **2012**, *46*, (16), 8976-8983.
- 449 3. Richardson, S. D.; Fasano, F.; Ellington, J. J.; Crumley, F. G.; Buettner, K. M.; Evans, J. J.; Blount, B.
450 C.; Silva, L. K.; Waite, T. J.; Luther, G. W.; McKague, A. B.; Miltner, R. J.; Wagner, E. D.; Plewa, M. J.,
451 Occurrence and Mammalian Cell Toxicity of Iodinated Disinfection Byproducts in Drinking Water.
452 *Environ. Sci. Technol.* **2008**, *42*, (22), 8330-8338.
- 453 4. Westerhoff, P.; Chao, P.; Mash, H., Reactivity of natural organic matter with aqueous chlorine
454 and bromine. *Water Res.* **2004**, *38*, (6), 1502-1513.

- 455 5. Richardson, S. D.; Plewa, M. J.; Wagner, E. D.; Schoeny, R.; DeMarini, D. M., Occurrence,
456 genotoxicity, and carcinogenicity of regulated and emerging disinfection by-products in drinking water:
457 A review and roadmap for research. *Mutat Res-Rev Mutat.* **2007**, *636*, (1-3), 178-242.
- 458 6. P. Neta; V. Madhavan; Haya Zemel; Richard, W. F., Rate constants and mechanism of reaction of
459 sulfate radical anion with aromatic compounds. *J. Am. Chem. Soc.* **1977**, *99*, 163-164.
- 460 7. Furman, O. S.; Teel, A. L.; Watts, R. J., Mechanism of Base Activation of Persulfate. *Environ. Sci.*
461 *Technol.* **2010**, *44*, (16), 6423-6428.
- 462 8. Guan, Y. H.; Ma, J.; Li, X. C.; Fang, J. Y.; Chen, L. W., Influence of pH on the Formation of Sulfate
463 and Hydroxyl Radicals in the UV/Peroxymonosulfate System. *Environ. Sci. Technol.* **2011**, *45*, (21), 9308-
464 9314.
- 465 9. Johnson, R. L.; Tratnyek, P. G.; Johnson, R. O., Persulfate Persistence under Thermal Activation
466 Conditions. *Environ. Sci. Technol.* **2008**, *42*, (24), 9350-9356.
- 467 10. Anipsitakis, G. P.; Dionysiou, D. D., Radical generation by the interaction of transition metals
468 with common oxidants. *Environ. Sci. Technol.* **2004**, *38*, (13), 3705-3712.
- 469 11. Sun, J. H.; Li, X. Y.; Feng, J. L.; Tian, X. K., Oxone/Co²⁺ oxidation as an advanced oxidation process:
470 Comparison with traditional Fenton oxidation for treatment of landfill leachate. *Water Res.* **2009**, *43*,
471 (17), 4363-4369.
- 472 12. Deng, Y.; Eyzske, C. M., Sulfate radical-advanced oxidation process (SR-AOP) for simultaneous
473 removal of refractory organic contaminants and ammonia in landfill leachate. *Water Res.* **2011**, *45*, (18),
474 6189-6194.
- 475 13. Zhen, G. Y.; Lu, X. Q.; Li, Y. Y.; Zhao, Y. C.; Wang, B. Y.; Song, Y.; Chai, X. L.; Niu, D. J.; Cao, X. Y.,
476 Novel insights into enhanced dewaterability of waste activated sludge by Fe(II)-activated persulfate
477 oxidation. *Bioresour. Technol.* **2012**, *119*, 7-14.
- 478 14. Anipsitakis, G. P.; Tufano, T. P.; Dionysiou, D. D., Chemical and microbial decontamination of
479 pool water using activated potassium peroxymonosulfate. *Water Res.* **2008**, *42*, (12), 2899-2910.
- 480 15. Neta, P.; Huie, R. E.; Ross, A. B., Rate constants for reactions of inorganic radicals in aqueous-
481 solution. *J. Phys. Chem. Ref. Data* **1988**, *17*, (3), 1027-1284.
- 482 16. Yu, X. Y.; Bao, Z. C.; Barker, J. R., Free radical reactions involving Cl-center dot, Cl-2(-center dot),
483 and SO4-center dot in the 248 nm photolysis of aqueous solutions containing S₂O₈²⁻ and Cl. *J. Phys. Chem.*
484 *A.* **2004**, *108*, (2), 295-308.
- 485 17. Zehavi, D.; Rabani, J., Oxidation of aqueous bromide ions by hydroxyl radicals. Pulse radiolytic
486 investigation. *J. Phys. Chem.* **1972**, *76*, (3), 312-&.
- 487 18. Neta, P.; Huie, R. E.; Ross, A. B., Rate constants for reactions of inorganic radicals in aqueous
488 solution. *J. Phys. Chem. Ref. Data* **1988**, *17*, (3), 1027-1284.
- 489 19. Von Gunten, U.; Oliveras, Y., Advanced oxidation of bromide-containing waters: Bromate
490 formation mechanisms. *Environ. Sci. Technol.* **1998**, *32*, (1), 63-70.
- 491 20. Avner Mamou; Rabanl, J.; Behar, D., Oxidation of aqueous bromide(1-) by hydroxyl radicals,
492 studies by pulse radiolysis. *J. Phys. Chem.* **1977**, *81*, (15), 1447-1448.
- 493 21. Beckwith, R. C.; Wang, T. X.; Margerum, D. W., Equilibrium and kinetics of bromine hydrolysis.
494 *Inorg. Chem.* **1996**, *35*, (4), 995-1000.
- 495 22. Fortnum, D. H.; Battaglia, C. J.; Cohen, S. R.; Edwards, J. O., The kinetics of oxidation of halide
496 ions by monosubstituted peroxides. *J. Am. Chem. Soc.* **1960**, *82*, (4), 778-782.
- 497 23. Croué, J. P.; Korshin, G. V.; Benjamin, M. M., *Characterization of natural organic matter in*
498 *drinking water*. AWWA Research Foundation: USA, 2000.
- 499 24. Zhang, T.; Zhu, H.; Croue, J.-P., Production of Sulfate Radical from Peroxymonosulfate Induced
500 by a Magnetically Separable CuFe₂O₄ Spinel in Water: Efficiency, Stability, and Mechanism. *Environ. Sci.*
501 *Technol.* **2013**, *47*, (6), 2784-2791.

- 502 25. Hwang, C. J.; Krasner, S. W.; Scilimenti, M. J.; Amy, G. L.; Dickenson, E.; Bruchet, A.; Prompsy, C.;
503 Gisele, F.; Croué, J. P.; Violleau, D.; Leenheer, J. *Polar NOM : Characterization , DBPs, Treatment*; the
504 AWWA Research Foundation and American Water Works Association: USA, 2001.
- 505 26. Lutze, H. V.; Bakkour, R.; Kerlin, N.; von Sonntag, C.; Schmidt, T. C., Formation of bromate in
506 sulfate radical based oxidation: Mechanistic aspects and suppression by dissolved organic matter. *Water*
507 *Res.* **2014**, *53*, 370-377.
- 508 27. Rastogi, A.; Ai-Abed, S. R.; Dionysiou, D. D., Sulfate radical-based ferrous-peroxymonosulfate
509 oxidative system for PCBs degradation in aqueous and sediment systems. *Appl. Catal. B-Environ.* **2009**,
510 *85*, (3-4), 171-179.
- 511 28. Singer, P. C. In *Basin Concepts of Disinfection By-Product Formation and Control*, AWWA D/DBP
512 Rule Teleconference, Presentation 1, **1993**, pp 1-20.
- 513 29. Hua, G. H.; Reckhow, D. A., DBP formation during chlorination and chloramination: Effect of
514 reaction time, pH, dosage, and temperature. *J. Am. Water Work Assoc.* **2008**, *100*, (8), 82-+.
- 515 30. Krasner, S. W.; Weinberg, H. S.; Richardson, S. D.; Pastor, S. J.; Chinn, R.; Scilimenti, M. J.; Onstad,
516 G. D.; Thruston, A. D., Jr., Occurrence of a new generation of disinfection byproducts. *Environ. Sci.*
517 *Technol.* **2006**, *40*, (23), 7175-7185.
- 518 31. Hua, G. H.; Reckhow, D. A.; Kim, J., Effect of bromide and iodide ions on the formation and
519 speciation of disinfection byproducts during chlorination. *Environ. Sci. Technol.* **2006**, *40*, (9), 3050-3056.
- 520 32. Kristiana, I.; Gallard, H.; Joll, C.; Croue, J.-P., The formation of halogen-specific TOX from
521 chlorination and chloramination of natural organic matter isolates. *Water Res.* **2009**, *43*, (17), 4177-4186.
- 522 33. Diehl, A. C.; Speitel, G. E.; Symons, J. M.; Krasner, S. W.; Hwang, C. J.; Barrett, S. E., DBP
523 formation during chloramination. *J. Am. Water Works Assoc.* **2000**, *92*, (6), 76-90.
- 524 34. Madhavan, V.; Levanon, H.; Neta, P., Decarboxylation by $SO_4^{\cdot-}$ radicals. *Radiat. Res.* **1978**, *76*,
525 12-22.
- 526 35. Grgic, I.; Podkrajsek, B.; Barzaghi, P.; Herrmann, H., Scavenging of $SO_4^{\cdot-}$ radical anions by mono-
527 and dicarboxylic acids in the Mn(II)-catalyzed S(IV) oxidation in aqueous solution. *Atmos. Environ.* **2007**,
528 *41*, (39), 9187-9194.
- 529 36. Larson, R. A.; Rockwell, A. L., Citric acid: Potential precursor of chloroform in water chlorination.
530 *Naturwissenschaften* **1978**, *65*, (9), 490-490.
- 531 37. Dickenson, E. R. V.; Summers, R. S.; Croue, J.-P.; Gallard, H., Haloacetic acid and trihalomethane
532 formation from the chlorination and bromination of aliphatic beta-dicarbonyl acid model compounds.
533 *Environ. Sci. Technol.* **2008**, *42*, (9), 3226-3233.
- 534 38. Reckhow, D. A.; Singer, P. C., *Mechanisms of organic halide formation during fulvic acid*
535 *chlorination and implications with respect to preozonation*. Lewis publishers, Inc.: Chelsea, Michigan,
536 1985; Vol. 5.
- 537 39. Antoniou, M. G.; de la Cruz, A. A.; Dionysiou, D. D., Intermediates and Reaction Pathways from
538 the Degradation of Microcystin-LR with Sulfate Radicals. *Environ. Sci. Technol.* **2010**, *44*, (19), 7238-7244.
- 539 40. Weiss, H., Aqueous bromination of maleate and fumarate ions. *J. Am. Chem. Soc.* **1977**, *99*, (5),
540 1670-1672.
- 541 41. Bond, T.; Henriot, O.; Goslan, E. H.; Parsons, S. A.; Jefferson, B., Disinfection Byproduct
542 Formation and Fractionation Behavior of Natural Organic Matter Surrogates. *Environ. Sci. Technol.* **2009**,
543 *43*, (15), 5982-5989.
- 544 42. Shah, A. D.; Mitch, W. A., Halonitroalkanes, Halonitriles, Haloamides, and N-Nitrosamines: A
545 Critical Review of Nitrogenous Disinfection Byproduct Formation Pathways. *Environ. Sci. Technol.* **2012**,
546 *46*, (1), 119-131.
- 547 43. Huang, H.; Wu, Q. Y.; Hu, H. Y.; Mitch, W. A., Dichloroacetonitrile and Dichloroacetamide Can
548 Form Independently during Chlorination and Chloramination of Drinking Waters, Model Organic Matters,
549 and Wastewater Effluents. *Environ. Sci. Technol.* **2012**, *46*, (19), 10624-10631.

- 550 44. Hureiki, L.; Croue, J. P.; Legube, B., Chlorination studies of free and combined amino acids.
551 *Water Res.* **1994**, *28*, (12), 2521-2531.
- 552 45. Gallard, H.; Allard, S.; Nicolau, R.; von Gunten, U.; Croue, J. P., Formation of Iodinated Organic
553 Compounds by Oxidation of Iodide-Containing Waters with Manganese Dioxide. *Environ. Sci. Technol.*
554 **2009**, *43*, (18), 7003-7009.
- 555 46. Sra, K. S.; Thomson, N. R.; Barker, J. F., Persulfate injection into a gasoline source zone. *J.*
556 *Contam. Hydrol.* **2013**, *150*, 35-44.
- 557

Table 1. Formation of TOBr and Br-DBPs from Model Compounds

Compound	TOBr ($\mu\text{g L}^{-1}$)		DBAA ($\mu\text{g L}^{-1}$)		MBAA ($\mu\text{g L}^{-1}$)		TBAA ($\mu\text{g L}^{-1}$)		TBM ($\mu\text{g L}^{-1}$)		DBAN ($\mu\text{g L}^{-1}$)		DBAcAm ($\mu\text{g L}^{-1}$)		BAcAm ($\mu\text{g L}^{-1}$)	
	$\text{SO}_4^{*}/\text{Br}^-$	HOBr	$\text{SO}_4^{*}/\text{Br}^-$	HOBr	$\text{SO}_4^{*}/\text{Br}^-$	HOBr	$\text{SO}_4^{*}/\text{Br}^-$	HOBr	$\text{SO}_4^{*}/\text{Br}^-$	HOBr	$\text{SO}_4^{*}/\text{Br}^-$	HOBr	$\text{SO}_4^{*}/\text{Br}^-$	HOBr	$\text{SO}_4^{*}/\text{Br}^-$	HOBr
Group I																
L-Asparagine	294.0	1574.2	126.3	233.3	1.1	1.0	ND	ND	ND	ND	2.4	112.9	117.4	1068.6	14.0	ND
L-Glutamic acid	93.0	77.3	17.0	0.16	1.8	ND	ND	ND	0.8	0.090	2.9	1.83	6.1	5.0	4.1	ND
L-Phenylalanine	48.9	61.5	4.1	0.16	1.9	ND	ND	ND	1.0	ND	2.7	2.19	4.5	5.0	3.8	ND
L-Tryptophan	165.8	153.0	2.0	0.65	1.4	ND	ND	ND	ND	4.39	2.3	1.92	4.5	11.3	3.9	ND
L-Tyrosine	1406.2	1302.6	5.9	1.6	1.5	ND	ND	6.1	0.2	85.6	2.4	2.5	4.8	6.9	3.4	ND
L-aspartic acid	609.5	393.9	198.3	0.71	18.3	ND	ND	ND	15.2	36.30	29.2	5.8	6.5	6.3	ND	ND
Group II																
Phenol	1069.0	1988.5	2.8	0.25	0.2	ND	ND	4.0	ND	141.2	NA	NA	NA	NA	NA	NA
Hydroquinone	163.2	314.6	19.1	1.85	1.9	ND	ND	5.5	9.3	32.5	NA	NA	NA	NA	NA	NA
Salicylic acid	1694.2	2054.2	28.9	0.70	1.4	ND	ND	3.4	17.2	51.0	NA	NA	NA	NA	NA	NA
Group III																
Citric acid	1435.0	1185.8	434.6	198.5	85.3	9.9	1.9	4.0	1144.3	966.3	NA	NA	NA	NA	NA	NA
Oxalic acid	147.0	91.5	0.5	0.090	ND	ND	ND	ND	4.6	23.8	NA	NA	NA	NA	NA	NA
Malonic acid	59.4	652.6	8.7	488.1	3.2	20.5	ND	ND	15.9	0.59	NA	NA	NA	NA	NA	NA
Succinic acid	601.1	60.3	14.0	0.12	1.7	ND	4.3	ND	606.9	52.8	NA	NA	NA	NA	NA	NA
Maleic acid	324.9	762.7	3.6	0.15	0.1	ND	2.6	4.6	149.2	30.2	NA	NA	NA	NA	NA	NA
Pyruvic acid	395.0	261.4	29.7	0.69	2.5	2.9	ND	ND	396.4	278.9	NA	NA	NA	NA	NA	NA

Note: Incorporation of bromine into model compounds by SR-AOP: PMS = 100 μM ; CuFe_2O_4 dose = 50 mg L^{-1} ; bromide = 50 μM ; model compound = 50 μM ; pH=8.0 in 10 mM tetraborate buffer; contact time 24 h. Bromination of model compounds: HOBr/OBr⁻ = 50 μM ; model compound = 50 μM ; pH=8.0 in 10 mM tetraborate buffer; contact time 24 h. The results are the average values of duplicate tests. ND: not detected; NA: not applicable.

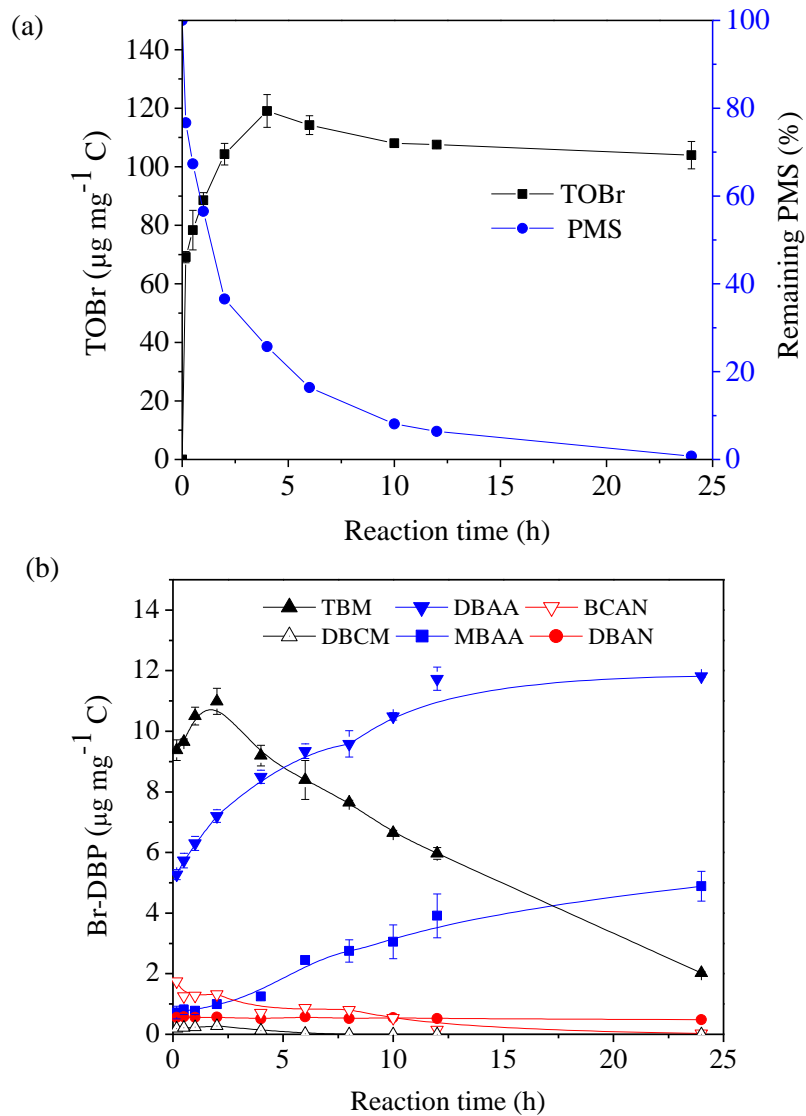


Figure 1. Kinetics of TOBr and Br-DBPs formation from bromide-containing water by SR-AOP:

(a) decomposition of PMS and evolution profile of TOBr; (b) evolution profiles of Br-DBP.

Experimental conditions: 5 mg solid SR HPOA per liter MQ (2.25 mg L⁻¹ DOC); PMS = 50 μM ;

CuFe₂O₄ = 50 mg L⁻¹; Br⁻ = 25 μM ; T = 20 °C; pH = 7.5.

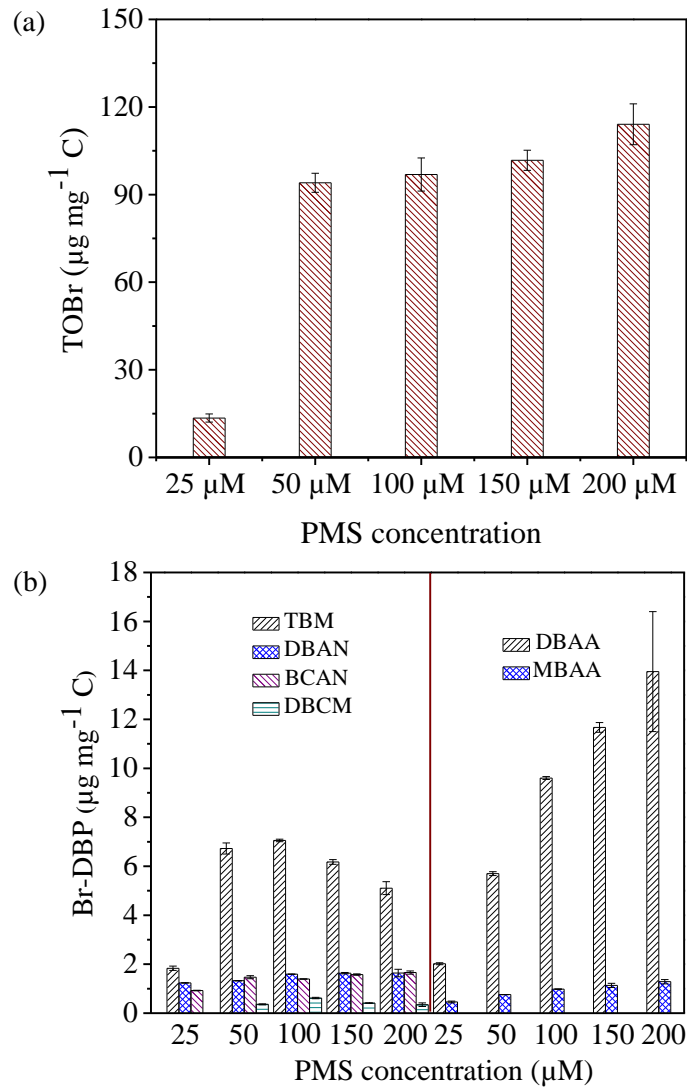


Figure 2. Effect of PMS concentration on the formation and speciation of TOBr and Br-DBPs by SR-AOP: (a) Bromine incorporation into TOBr; (b) THMs, HANs, and HAAs speciation.

Experimental conditions: 5 mg solid SR HPOA per liter MQ ($2.25 \text{ mg L}^{-1} \text{ DOC}$); $\text{CuFe}_2\text{O}_4 = 50 \text{ mg L}^{-1}$; $\text{Br}^- = 25 \text{ }\mu\text{M}$; contact time = 2 h; $T = 20 \text{ }^\circ\text{C}$; $\text{pH} = 5.5$.

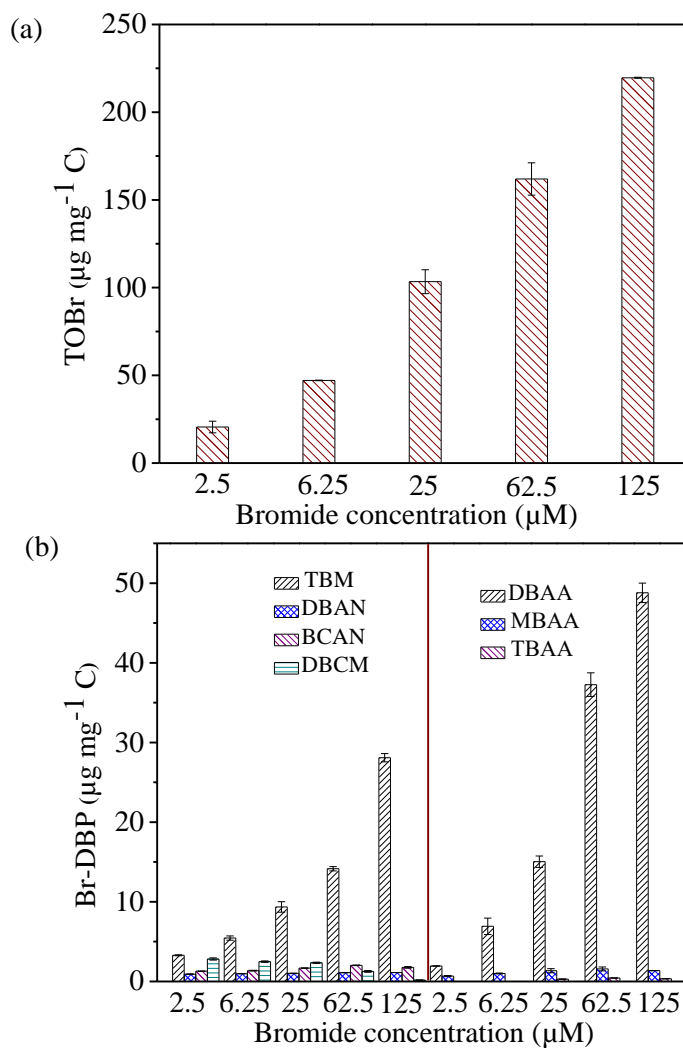


Figure 3. Bromine incorporation into TOBr and Br-DBPs under various bromide concentrations: (a) Bromine incorporation into TOBr; (b) THMs, HANs, and HAAs speciation. Experimental conditions: 5 mg solid SR HPOA per liter MQ ($2.25 \text{ mg L}^{-1} \text{ DOC}$); PMS = $100 \mu\text{M}$; $\text{CuFe}_2\text{O}_4 = 50 \text{ mg L}^{-1}$; contact time = 2 h; $T = 20 \text{ }^\circ\text{C}$; $\text{pH} = 7.5$

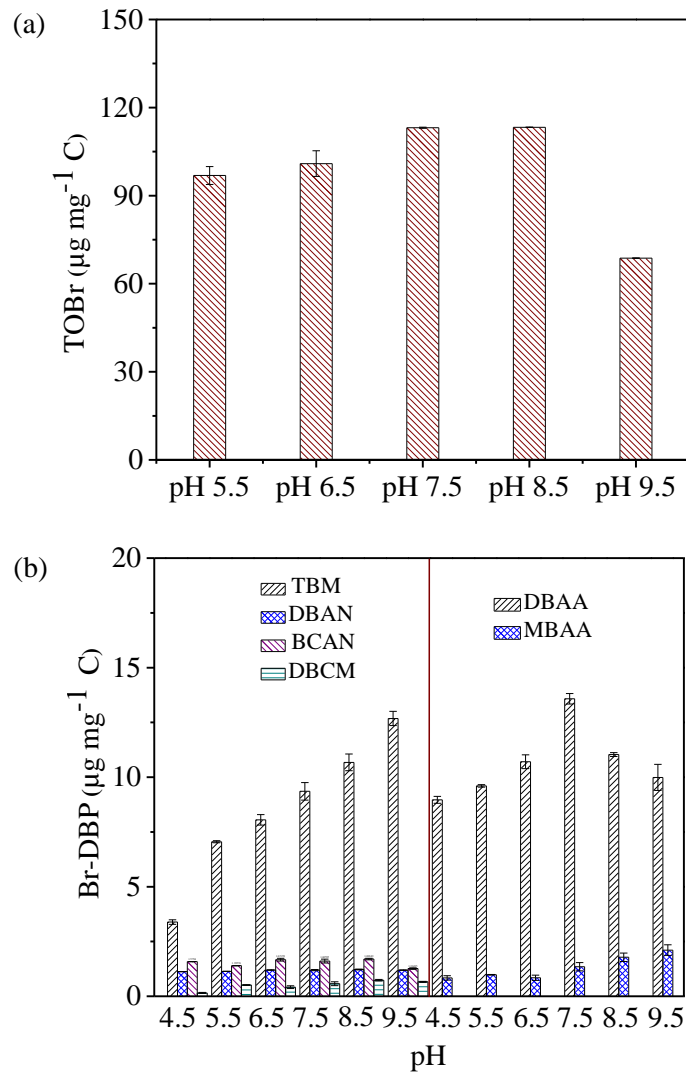


Figure 4. Effect of solution pH on the formation and speciation of TOBr and Br-DBPs by SR-AOP: (a) Bromine incorporation into TOBr; (b) THMs, HANs, and HAAs speciation.

Experimental conditions: 5 mg solid SR HPOA per liter MQ ($2.25 \text{ mg L}^{-1} \text{ DOC}$); PMS = 100 μM ; $\text{CuFe}_2\text{O}_4 = 50 \text{ mg L}^{-1}$; bromide = 25 μM ; contact time = 2 h; $T = 20 \text{ }^\circ\text{C}$.

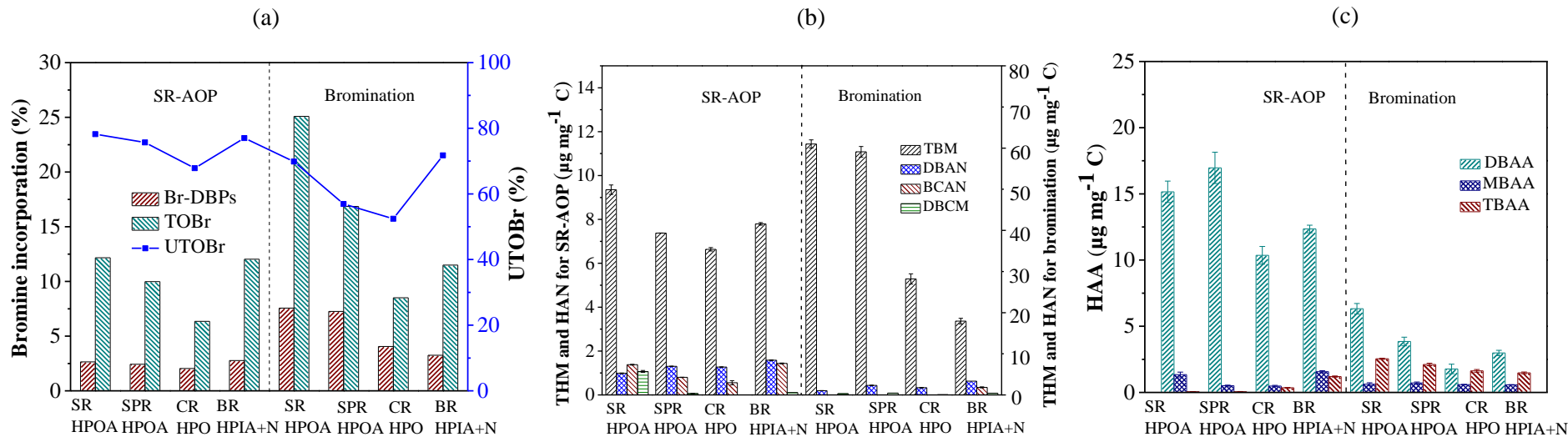


Figure 5. Formation and speciation of TOBr and Br-DBPs from NOM isolates by SR-AOP and bromination: (a) Proportion of unknown compounds in TOBr (UTOBr) and bromine incorporation into TOBr and Br-DBPs; (b) THMs and HANs speciation; (c) HAAs speciation. Experimental conditions: 5 - 7 mg solid NOM isolate per liter MQ; pH = 7.5; contact time = 2 h; T = 20 °C; for SR-AOP, PMS = 100 µM, CuFe₂O₄ = 50 mg L⁻¹, Br⁻ = 25 µM; for bromination, HOBr/OBr⁻ = 25 µM.